

3D Fiber Orientation and Warpage Analysis of Injection-Molded Throttle Valve

Allen Peng*, Yorker Chang, Anthony Yang and Venny Yang
CoreTech System Co.,Ltd., Hsin-Chu 30043, Taiwan

Fu Chin Chuang
DSM Engineering Plastics

Abstract

A lot of automobile plastic parts are made of fiber-reinforced engineering plastic for its superior mechanical properties and high heat distortion temperature. The fiber orientation and anisotropy shrinkage in injection molding are complex 3D phenomena. They are difficult to identify and study by the traditional 2.5D model. The thermal and mechanics properties of the composite closely relate with the fiber orientation pattern. Thermal shrinkage is larger in transverse direction and lower in fiber orientation direction. This 3D technique is proved to be a powerful tool for the study of 3D fiber orientation and anisotropy shrinkage phenomena and a cost-effective approach for related part/mold designers.

Introduction

The fiber-reinforced composite products with stiffness properties are usually superior to those of unreinforced polymer products. For the recent years, the injection molding of fiber-reinforced thermoplastics has been very popular. A lot of automobile plastic parts are made of fiber-reinforced engineering plastic for its superior mechanical properties and high heat distortion temperature. We know the injection molding of fiber-reinforced thermoplastics is a complicated process. The reinforced composites don't possess isotropic material properties. The thermal and mechanics properties of the composite strongly depend on the fiber orientation pattern. The composite is stronger in the fiber orientation direction and weaker in the transverse direction. In other word, the thermal shrinkage is larger in transverse direction and lower in fiber orientation direction. The molded product may have high internal stress and warpage at unexpected locations. Therefore, during the design phase of a new product, we must take account of processing details. So the fiber orientation and warpage behavior of the part can be effectively predicted.

The fiber orientation and anisotropic shrinkage in injection molding are complex 3D phenomena. It's difficult to identify and study by the traditional 2.5D model. When the fiber-reinforced polymer is injection molded, the flow during mold filling creates the pattern of fiber orientation in the part. This leads to anisotropy in the mechanics properties of material. Essentially, the fiber orientation is full 3D components. The direction of orientation may be the any direction in 3D domain. Only full 3D model can simulate an entire injection-molded part and get the complete distribution of fiber orientation.

Theory

The governing equations to simulate the 3D, transient, and non-isothermal polymer flow with free surface are as follows,

$$\frac{\partial \rho}{\partial t} + \nabla \cdot \rho \mathbf{u} = 0 \quad (1)$$

$$\frac{\partial}{\partial t}(\rho \mathbf{u}) + \nabla \cdot (\rho \mathbf{u} \mathbf{u} - \boldsymbol{\sigma}) = \rho \mathbf{g} \quad (2)$$

$$\boldsymbol{\sigma} = -p \mathbf{I} + \eta (\nabla \mathbf{u} + \nabla \mathbf{u}^T) \quad (3)$$

$$\rho C_p \left(\frac{\partial T}{\partial t} + \mathbf{u} \cdot \nabla T \right) = \nabla \cdot (\mathbf{k} \nabla T) + \Phi \quad (4)$$

In this paper, the fiber orientation state at each point in the part is represented by a 2nd-order orientation vector \mathbf{A} ,

$$A_{ij} = \int (p_i p_j) \varphi(p) dp \quad (6)$$

The equation of orientation change for the orientation tensor proposed by Advani and Tucker is employed for the analysis,

$$\frac{\partial A_{ij}}{\partial t} + u_k \frac{\partial A_{ij}}{\partial x_k} = A_{ik} \Omega_{kj} - \Omega_{ik} A_{kj} + \lambda (A_{ik} E_{kj} + E_{ik} A_{kj} - 2A_{ijkl} E_{kl}) + 2C_I \dot{\gamma} (\delta_{ij} - 3A_{ij}) \quad (7)$$

where C_I is the interaction coefficient with the value ranged from 10^{-2} to 10^{-3} . For the fourth-order tensor A_{ijkl} , a closure approximation is needed.

Another important consequence of fiber orientation is the anisotropy in the macroscopic physical properties of the material. An elastic anisotropic material needs 21 constants for a full characterization.

Since the fiber orientation is three-dimensional in 3D filling analysis, we can employ the most general formulation for anisotropic material for 3D Warpage analysis. Integrate the 3D fiber orientation distribution with unidirectional fiber-reinforced composite into the anisotropic material. The stiffness matrix for the anisotropic material is

$$\sigma_m = \begin{bmatrix} C_{11} & C_{12} & C_{13} & C_{14} & C_{15} & C_{16} \\ & C_{22} & C_{23} & C_{24} & C_{25} & C_{26} \\ & & C_{33} & C_{34} & C_{35} & C_{36} \\ & & & C_{44} & C_{45} & C_{46} \\ & & & & C_{55} & C_{56} \\ & & & & & C_{66} \end{bmatrix} \epsilon_n$$

Symm.

where there are 21 constants for a full characterization. Element-average material properties are assigned to each element when calculating the anisotropic warpage behavior.

Results and discussion

A rectangular plate of 100x50x1 mm molded with glass-fiber reinforced PET is simulated. Fig.1 shows the part geometry and the filling pattern. The gate is located in the center of the plate. Fig.2 displays the fiber orientation on the different cut planes. The orientation of the lines indicates the most favorable orientation direction and the color of each line represents the degree of orientation. In the vicinity of mold wall, we can see that the shearing flow tends to align the fibers along the flow. In the center cut plane, the flow is shear free and hence the fiber orientation is perpendicular to the flow direction. In Fig.3, the prediction shows the fiber alignment along the welding line. These analysis results agree well with the experimental observation.

Figure 4 and Figure 5 show the filling analysis results of rectangular plate. The resin uses ABS 15% glass-fiber filled. In the post-processing of fiber orientation, the biggest eigenvalue and its corresponding eigenvector are plotted together to show the complex fiber orientation phenomena. The orientation of the vector shows the most favorable orientation

direction, while the magnitude of it shows the degree of orientation. According to the orientation distribution and flow-induced volumetric shrinkage, we further simulate the anisotropic warpage, as shown in Figure 6.

Several industrial parts of complex geometries also are analyzed to demonstrate the capabilities of proposed three-dimensional approach. Figure 7 shows the throttle valve, which is the control unit of airflow. The dimension of air hole is very important for this automobile plastic part. So the warpage control in injection molding will be the key point. Figure 8 show the its CAE model, the number of element is 536,355. The resin is PET 35% glass-fiber filled. Besides, the model is hard to define its mid-plane. Only 3D analysis can provide accurate results. Figure 9 shows its cooling channel layout. Figure 10 shows the melt front at filling stage. Figure 11~13 show the fiber orientation distribution. Figure 14 show the temperature distribution at the end of cooling. Figure 15~16 show the fiber-induced anisotropic properties. Figure 17 shows the total deformation of warpage. Figure 18 shows the deformation of fiber orientation effect. We can clearly see the influence of fiber orientation effect from these results. Moreover, we can apply these results to change design or find out proper process condition. Figure 19~28 show the results of other industrial cases.

Conclusions

In the past, due to the poor hardware demands, it is difficult to simulate an entire injection-molded part using a 3D model. With the hardware progress, anyway it is not a dream to simulate full 3D analysis. This 3D fiber orientation analysis technique is proved to be a powerful tool for the study of 3D fiber orientation phenomena and fiber-induced anisotropic material. The integration of 3D fiber orientation analysis and 3D warpage analysis will be provided a cost-effective total solution for related part/mold designers.

References

1. E.C.Bernhardt (Ed.), "Computer Aided Engineering for Injection Molding", Hanser (1983)

2. T. Manzione (Ed.), "Applications of Computer Aided Engineering in Injection Molding", Hanser (1987)
3. C.L. Tucker III (Ed.), "Fundamentals of Computer Modeling for Polymer Processing", Hanser (1989)
4. V.W. Wang, C.A. Hieber, and K.K. Wang, *J. Polym. Eng.*, 7, 21, (1986)
5. G. Potsch and W. Michaeli, "The prediction of linear shrinkage and warpage for thermoplastic injection mouldings", 355, ANTEC 1990 (1990)
6. Takaaki Matsuoka, Jum-Ichi Takabatake, Akihiko Koiwai, Yoshinori Inoue, Satoru Yamamoto and Hideroh Takahashi, "Integrated simulation to predict warpage of injection molded parts", *Polymer Engineering and Science*, 31, 14 (1991)
7. Tim A. Osswald, "A finite element analysis of the thermomechanical behavior of fiber reinforced composites", *J. Thermoplastic Composite Material*, vol. 4 (1991)
8. J.X. Rietveld and S. -J. Liu, "Simulation of warpage caused by thermal and geometric asymmetries in injection molded articles", 1349, ANTEC 1992 (1992)
9. P. Kennedy, "Flow Analysis Reference Manual", Moldflow Pty. Ltd., Hanser (1993)
10. Y.W. Lo, D.D. Reible, J. Collier and C.H. Chen, *Polym. Eng. Sci.*, 43, 1393 (1994)
11. W.B. Young, *Polym. Composites*, 15, 118 (1994)
12. Hiroshi Koresawa, Jiroschi Suzuki, Tatsuo Takenaka and Seijun Kinjo, "Computational analysis of mold and die deformation during injection molding", *Proc. 3rd ICTDM, Taiwan* (1995)
13. V. Rajupalem, K. Talwar, and C. Friedl, 670, ANTEC 1997, Toronto (1997)
14. "Flow-induced alignment in composite materials", ed. by T.D. Papathansiou and D.C. Guell, Cambridge (1997).
15. J.F. Hetu, D.M. Gao, A. Garcia-Rejon, and G. Salloum, *Polym. Eng. Sci.*, 38, 223 (1998)
16. W. A. Rider and D. B. Kothe, *J. Comput. Phys.*, 141, 112 (1998)
17. K. M. B. Jansen, D. J. Van Dijk, and M. J. A. Freriksen, "Shrinkage anisotropy in fiber reinforced injection molded products", *Polymer Composites*, Vol. 19, No. 4 (1998)
18. R. Zheng, P. Kennedy, N. Phan-Thien, and X-J. Fan, "Thermoviscoelastic simulation of thermally and pressure-induced stress in injection moulding for the prediction of shrinkage and warpage for fiber-reinforced thermoplastics", *J. Non-Newtonian Fluid Mech.* (1999)
19. Brent E. VerWeyst, Charles L. Tucker III, Peter H. Foss, and John F. O'Gara, "Fiber orientation in 3-D injection molded features: prediction and experiment", submitted to *Int. Polymer Processing* (1999)
20. R.Y. Chang and W.H. Yang, "Numerical Simulation of Mold Filling in Injection Molding Using a Three-Dimensional Finite Volume Approach", submitted to *Int. J. Numer. Methods Fluids* (2000)
21. R.Y. Chang and W.H. Yang, "A Novel Three-Dimensional Analysis of Polymer Injection Molding", 740, ANTEC 2001, Dallas (2001)

Key words: Three-Dimensional, Injection Molding, Fiber orientation, Throttle valve, anisotropic warpage

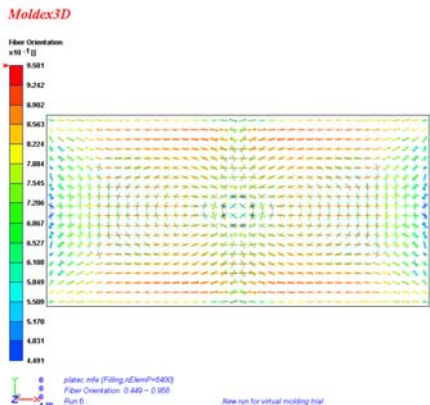
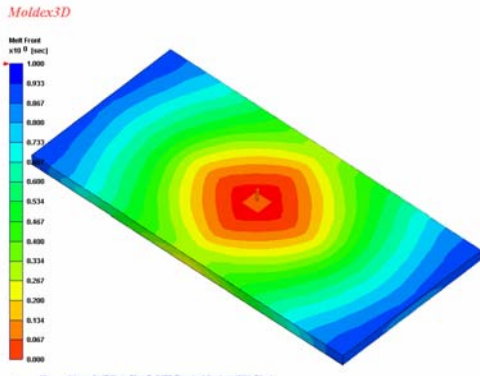


Figure 1. Melt front and fiber orientation

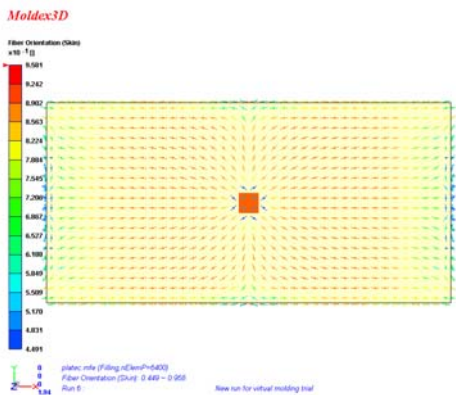


Figure 2 Fiber orientation on the wall (left) and in the center cut plane (right)

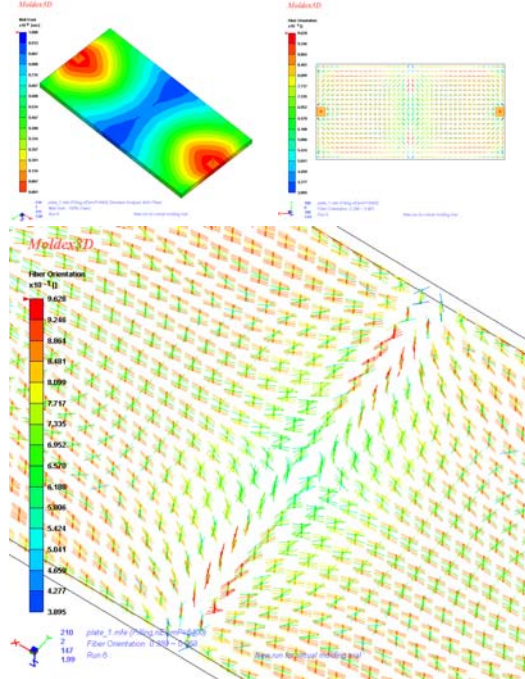
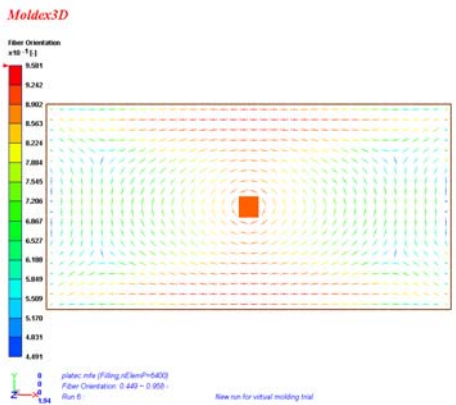


Figure 3. Melt front and fiber orientation on the welding line

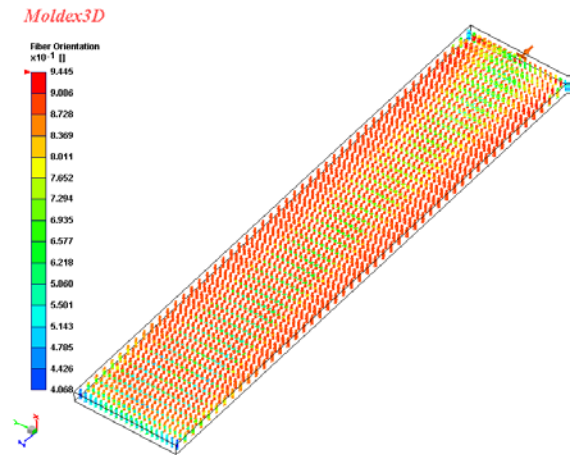


Figure 4. Fiber orientation distribution of rectangular plate

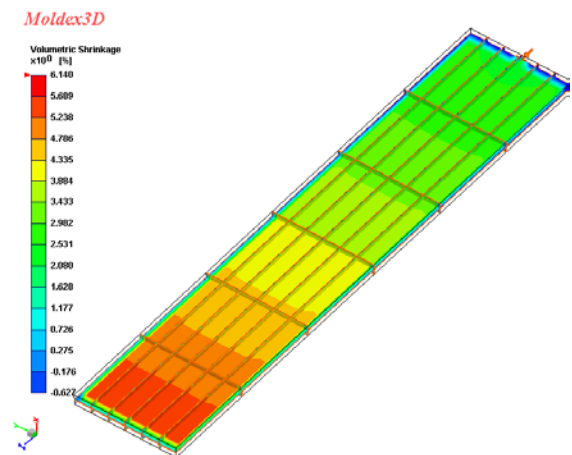


Figure 5. Volumetric shrinkage of rectangular plate at EOF

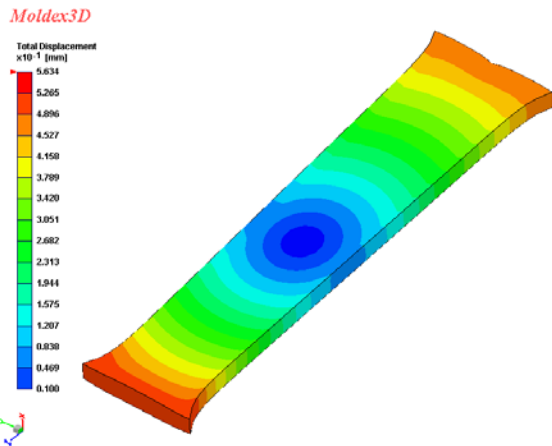


Figure 6. Warpage of rectangular plate

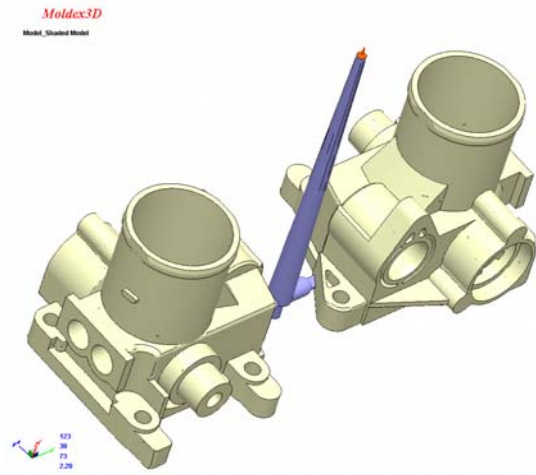


Figure 8. Throttle valve model



Figure 7. Throttle Valve (From DSM Engineering Plastics Korea)

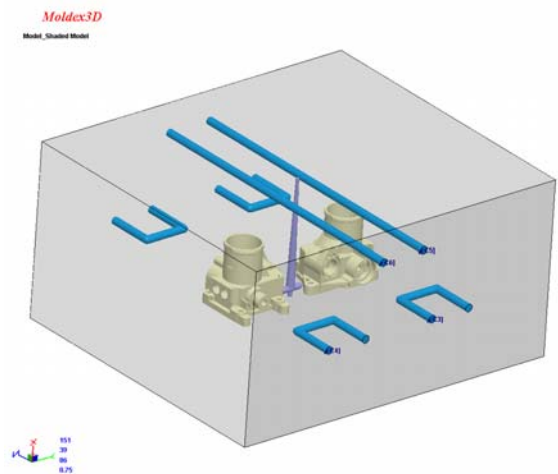


Figure 9. The cooling system of throttle valve

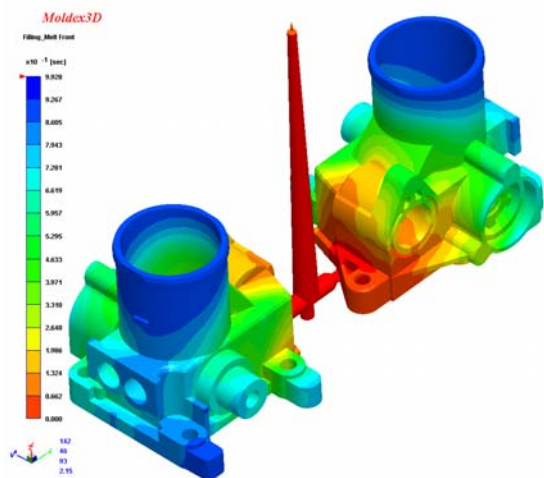


Figure 10. The filling melt front of throttle valve

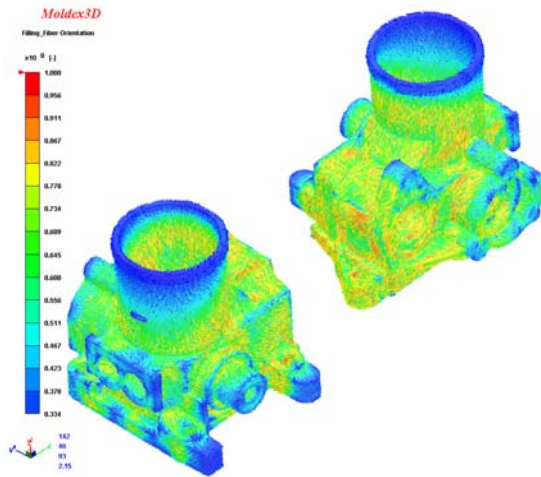


Figure 11. The fiber orientation distribution inside cavity at the end of filling

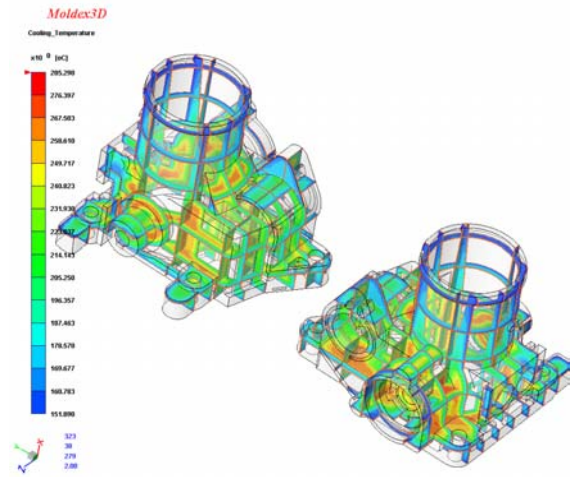


Figure 14. The temperature distribution inside cavity at the end of cooling

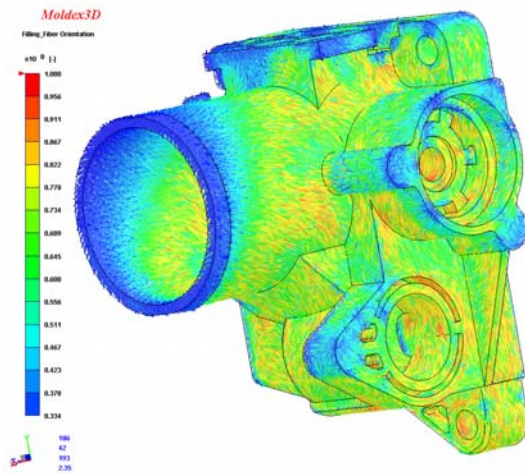


Figure 12. The fiber orientation distribution inside cavity at the end of filling

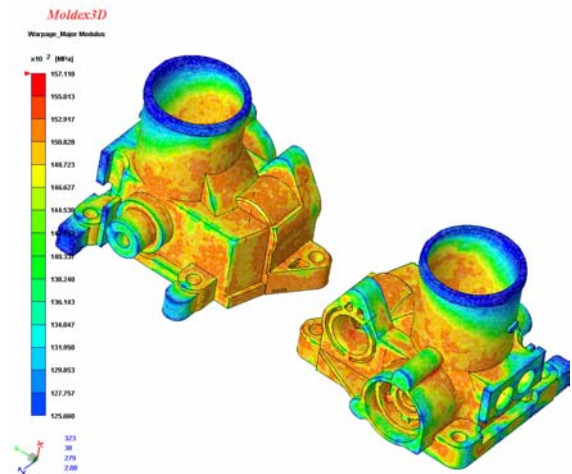


Figure 15. The fiber-induced major module distribution

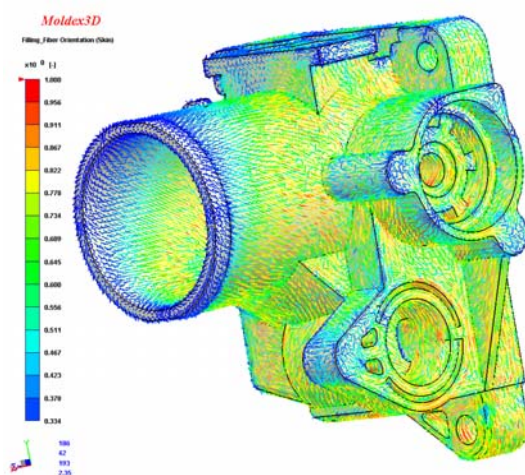


Figure 13. The fiber orientation distribution on cavity surface at the end of filling

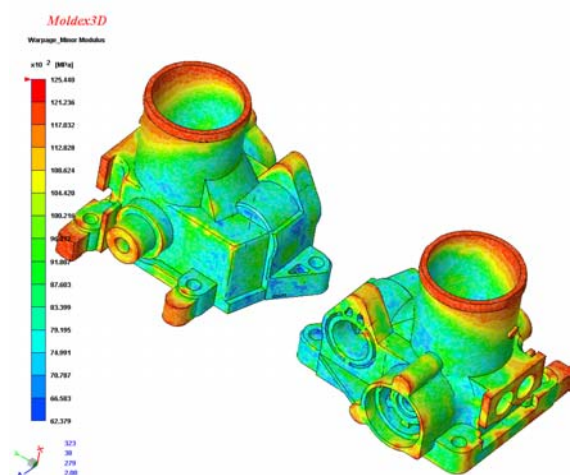


Figure 16. The fiber-induced minor module distribution

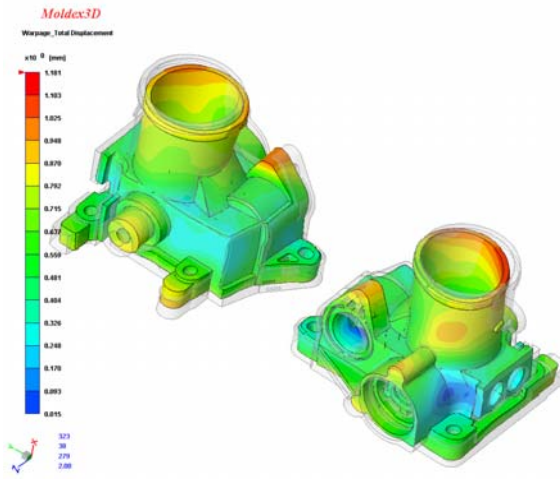


Figure 17. The total deformation of warpage analysis

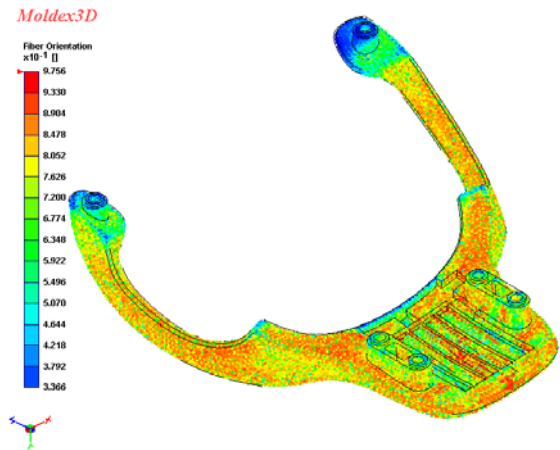


Figure 20. Fiber orientation distribution of motorcycle part

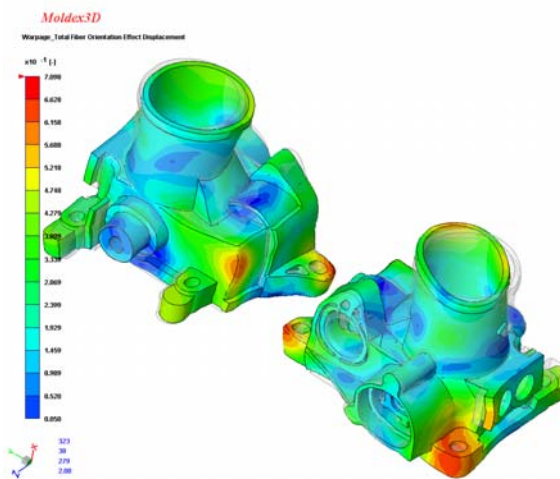


Figure 18. The fiber orientation effect deformation of warpage analysis

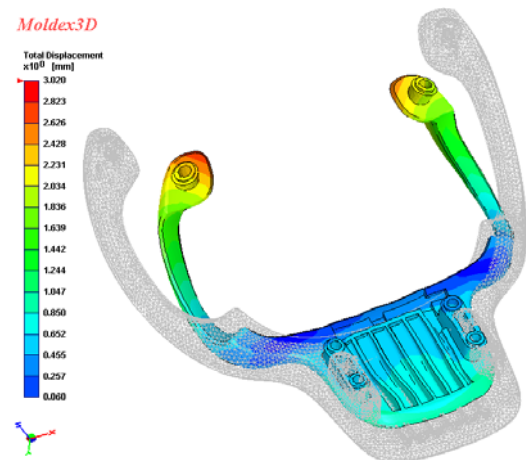


Figure 21. Warpage of motorcycle with fiber orientation effect

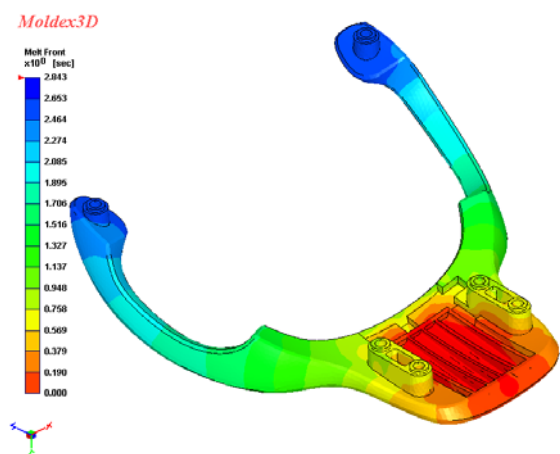


Figure 19. Filling results of motorcycle part

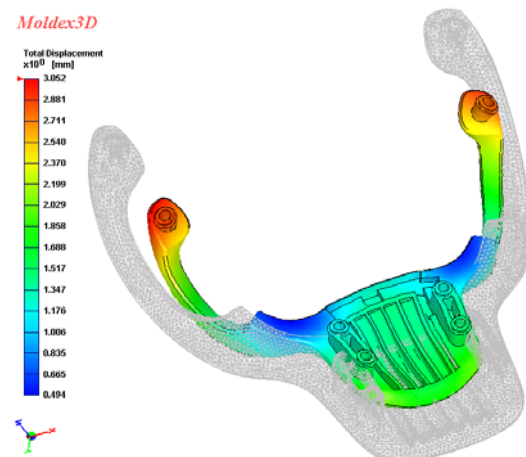


Figure 22. Warpage of motorcycle part without fiber orientation effect

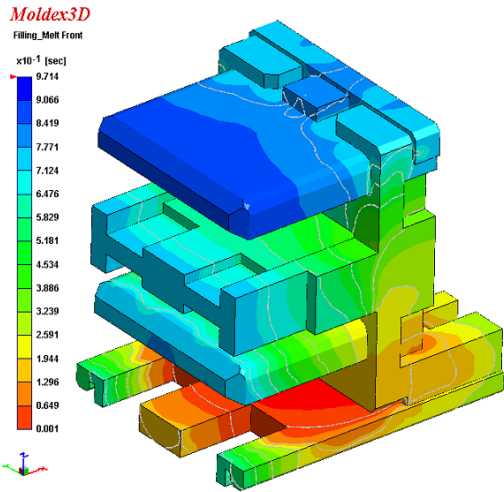


Figure 23. Filling results of connector

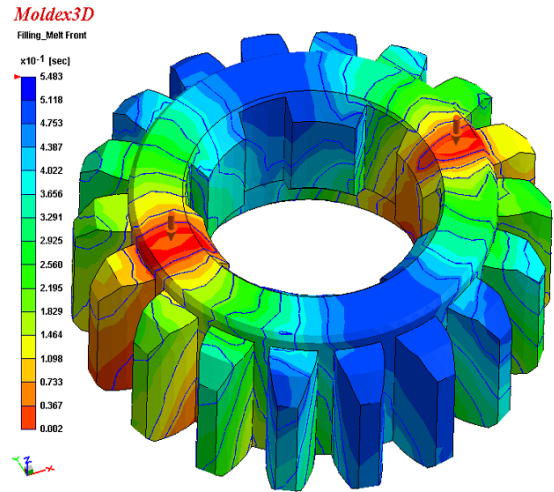


Figure 26. Filling results of gear

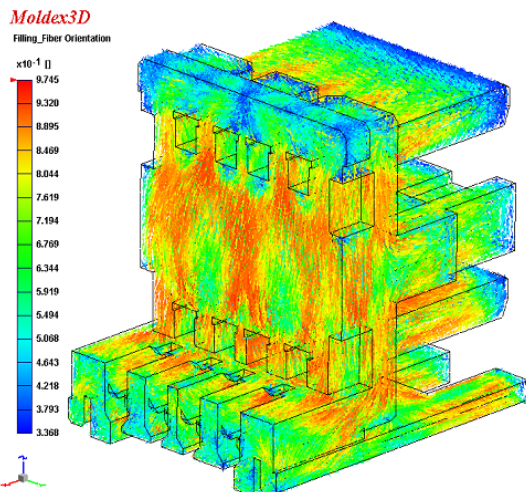


Figure 24. Fiber orientation distribution of connector

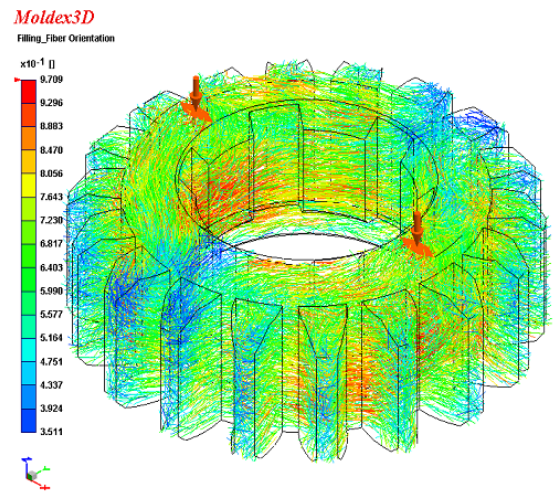


Figure 27. Fiber orientation distribution of gear

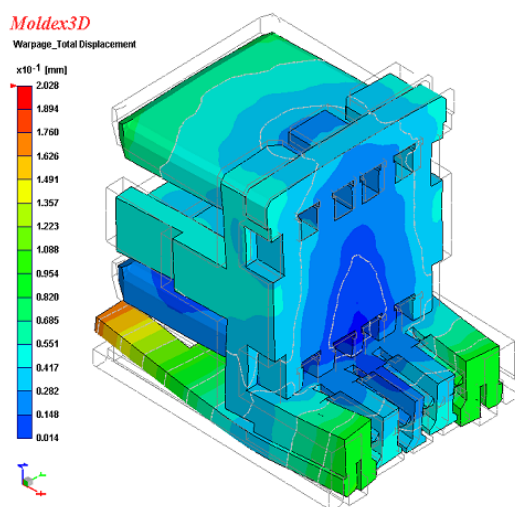


Figure 25. Warpage results of connector

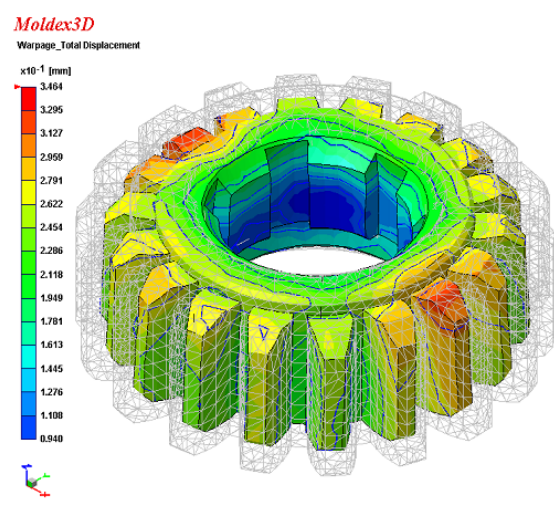


Figure 28. Warpage results of gear